Bioorganic & Medicinal Chemistry 18 (2010) 612–620

Contents lists available at ScienceDirect

Bioorganic & Medicinal Chemistry

journal homepage: www.elsevier.com/locate/bmc

Labeled 3-aryl-4-indolylmaleimide derivatives and their potential as angiogenic PET biomarkers

Ohad Ilovich, Hana Billauer, Sharon Dotan, Eyal Mishani *

Cyclotron/Radiochemistry Unit, Hadassah Hebrew University Hospital, Jerusalem 91120, Israel

ARTICLE INFO

Article history:
Received 21 October 2009
Revised 1 December 2009
Accepted 2 December 2009
Available online 6 December 2009

Keywords:
VEGFR-2
Carbon-11
PET
Angiogenesis

ABSTRACT

In a continued effort to find a suitable PET tracer for visualization of angiogenic processes, we explored the 3,4-diarylmaleimide family, known to have high affinity and selectivity towards the VEGFR-TKs. One previously reported agent and three new halogen-containing 3,4-diarylmaleimide derivatives were synthesized. The four maleimide derivatives were evaluated for their affinity and selectivity towards the VEGFRs and exhibited promising results. An automated carbon-11 radiolabeling route with a total synthesis time of 50 min successfully labeled the lead compound, resulting in 1.55 ± 0.15 GBq of tracer with a radiochemical yield of 20 ± 2%, 96% radiochemical purity and a SA of 111 ± 22 GBq/μmol (EOB, $n = 5$). The tracer possessed high stability in in vitro blood stability tests and specific VEGFR-TK binding profiles in intact cell binding experiments. Tracer lipophilicity was evaluated in an *n*-octanol/phosphate buffer system giving a Log $D_{7.4}$ of 1.99 ± 0.04. For the in vivo experiments, two animal models were used. The first was a U87 glioma tumor model, frequently reported in the literature and the second, a newly developed 293/KDR tumor model. Both models were validated for VEGFR-2 expression and used in in vivo biodistribution studies. These studies revealed low accumulation and rapid washout of the tracer from tumor tissue. High accumulation of activity in the liver prompted us to examine the tracer's in vitro stability to liver microsomes, revealing low resistance to P450 metabolism. In spite of encouraging in vitro results, the labeled lead tracer failed to accumulate in VEGFR-2 overexpressing tumors. It is possible that poor resistance to P450 metabolism reduces tracer's circulation leading to low tumor accumulation.

1. Introduction

Angiogenesis, the formation of new blood vessels from pre-existing vasculature, is a crucial mechanism for solid tumor growth and a key player in diseases such as arthritis, psoriasis and macular degeneration.[1] Angiogenesis is regulated by a balance of pro- and anti-angiogenic growth factors. Cognizant of the key roles angiogenesis plays in a multitude of pathological conditions, intensive research endeavors ensued to develop effective anti-angiogenic therapies.[2,3] These therapies include Avastin—a Vascular Endothelial Growth Factor (VEGF) scavenging antibody[4] and small molecule Vascular Endothelial Growth Factor Receptor (VEGFR) tyrosine kinase inhibitors (TKIs) such as sorafenib and sunitinib.[5]

Until recently, the only available end-points for traditional cytotoxic chemotherapy were factors such as tumor volume, time until relapse and patient survival. With increased understanding of cancer-related pathways, novel pharmacodynamic end-points for evaluating treatment efficacy at early stages are becoming available.[6] In the field of targeted therapies, knowledge regarding the expression and occupancy of different receptors before and during therapy could prove invaluable for evaluation of disease progression and therapy efficacy. One approach for obtaining this information is via molecular imaging such as Positron Emission Tomography (PET).[7]

Several potential targets for imaging angiogenesis, such as VEGF, its receptors and integrin αvβ3, have been investigated in the recent past. The RGD peptide motif, targeting integrin αvβ3, is the most studied angiogenic tracer. The labeling of RGD (both monomers and multimers) has been performed with several isotopes and various chemical structural changes were incorporated aimed at improving tracer pharmacokinetics.[8–10] Human studies have been initiated with some of these labeled peptides.[11]

The second potential family of targets for imaging angiogenesis is VEGF and its receptors. VEGFRs are members of the Receptor Tyrosine Kinase (RTK) superfamily and are composed of three major parts: an extracellular domain, a transmembrane region and an intracellular domain. The extracellular domain contains the ligand binding site. This domain has been a target for cancer therapy either directly using peptide antagonists[12] and anti-VEGFR antibodies[13] or indirectly using anti-VEGF antibodies.[14] The intracellular domain contains the tyrosine kinase domain which, when activated, initiates signal transduction pathways. This domain has been targeted using small molecule tyrosine kinase inhibitors

* Corresponding author. Tel.: +972 2 677 7931; fax: +972 2 6421203.
E-mail address: eyalmi@ekmd.huji.ac.il (E. Mishani).

0968-0896/$ - see front matter © 2009 Elsevier Ltd. All rights reserved.
doi:10.1016/j.bmc.2009.12.004

(TKIs). The development of imaging biomarkers targeting VEGF and its receptors has focused on the following approaches: labeling of anti-VEGF antibodies, labeling of VEGF isoforms and labeling of small molecule TKIs of VEGFR. A few anti-VEGF antibodies were labeled with ^{124}I, ^{111}In, and ^{89}Zr. These antibodies exhibited high variability in their distribution and clearance profiles and their tumor uptakes were low.[10] VEGF isoforms were labeled with $^{123/125}$I, ^{99m}Tc, ^{111}In, and ^{64}Cu. The iodinated isoforms had low tumor uptake and high thyroid uptake due to tracer degradation and release of free iodide.[15] The other labeled compounds gave mixed results, with one of the ^{64}Cu labeled isoforms exhibiting improved tumor uptake (~15%ID/g) and correlation between uptake and VEGFR-2 expression.[16]

Several small molecule TKIs were labeled and evaluated as potential tracers for noninvasive monitoring of angiogenic processes. A family of quinoline-ureas were labeled using fluorine-18[17] and carbon-11.[18] Their high Log *P* values could cause problems such as low specific tumor binding in vivo and high uptake in non-target tissues. Recently, an anilino-quinoline was labeled with carbon-11.[19] Although microPET studies yielded promising results, a stronger proof-of-concept such as specific and saturable binding in VEGFR-2 overexpressing tumors and data regarding the biodistribution of this tracer are lacking. In a continued effort to find a suitable tracer for evaluation of VEGFR-2 expression, we explored the 3,4-diarylmaleimide family[20,21] known to have high affinity and selectivity towards the tyrosine kinase domain of the VEGFR family.

2. Results and discussion

2.1. Chemistry

Three derivatives of the previously reported[20] VEGFR inhibitor **8**, with different halogen substituents were synthesized in order to allow for the future labeling with different PET radioisotopes. Synthesis was performed applying general methods described in the past with minor changes.[21,22] Briefly, the indoles were reacted with oxalyl chloride in an ethereal solution followed by addition of NaOMe in methanol to give four different indole-oxo-acetic esters **1–4** with yields of 56–85%.[22] 2-(3,4,5-trimethoxyphenyl)acetic acid was reacted with DCC and ammonia in a two-step, one-pot, overnight reaction to produce acetamide **5** with 80% yield. The acetamide was condensed with each of the four indole-oxo-acetic esters in THF using KO*t*Bu to furnish the four maleimide derivatives **8–11** with yields of 55–83% (Scheme 1). We found that the use of a 1:2 molar ratio of acetamide: indole-oxo-acetic esters gave good yields and little impurities for all four compounds. Lower ratios of indoles resulted in the formation of a multitude of by-products which were extremely hard to purify.

Our first choice for radiolabeling was the non-halogenated maleimide (**8**) published in the past. This compound can only be labeled using [^{11}C]CH_3I chemistry in a general route which could also be used to label the three other compounds. The synthesis of the desmethyl precursor molecule was performed using benzyl-protected phenyl acetic acid **6** which was amidated to give **7** under the same conditions used for compound **5** (yield 77%) and reacted with indole **1** to give the protected maleimide **12** with 73% yield. Compound **12** was deprotected using Pd/C under a hydrogen atmosphere to furnish the desmethyl maleimide precursor **13** (yield 67%) (Scheme 2).

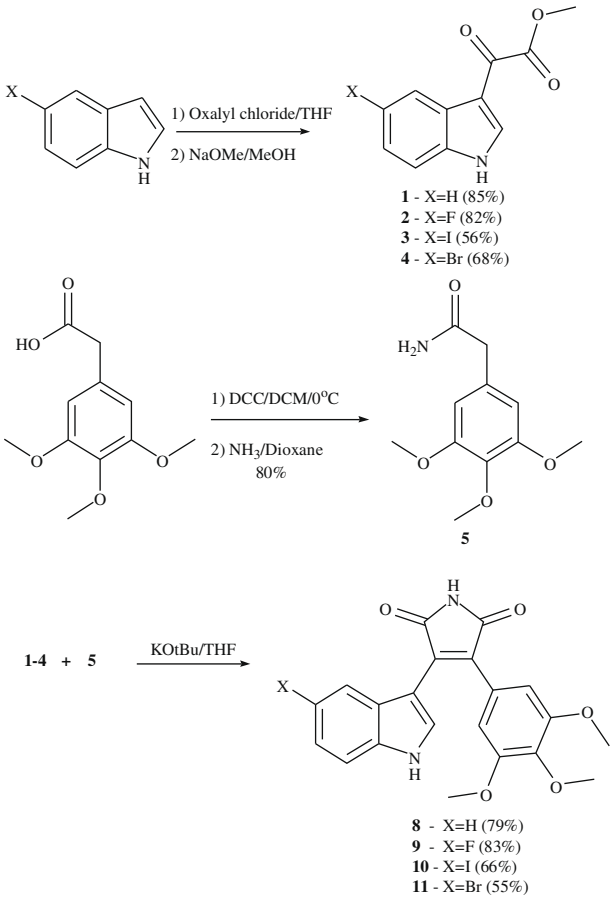

Scheme 1. Synthesis of maleimide derivatives.

2.2. Evaluation of IC_{50} values for inhibition of 10 tyrosine kinases

The four compounds were evaluated for their affinity and selectivity towards a family of relevant tyrosine kinases (Table 1). All four compounds showed high affinity and selectivity towards the three VEGFRs tested. IC_{50} values of 20–50 nM towards the three VEGFRs were obtained for compound **8** and good selectivity relative to the rest of the tested receptors. The presence of a fluorine atom on the indole ring was expected to decrease electron density, thus addressing stability problems which caused intramolecular cyclization during an agarose pellet production, and loss of receptor binding and biological activity.[21] However, during the synthesis of compound **9**, some cyclization still occurred, albeit to a lesser extent relative to the hydrogen analog. Compound **9** showed the least affinity towards the VEGFRs suggesting that high electron density in the indole ring is an important factor for receptor affinity. This may be manifested in hydrogen bonding between the secondary amine and the receptor's binding site. In addition, **9** had diminished selectivity towards the VEGFR-2 versus all other receptors with a loss of selectivity (defined as a ratio of 1:20 or less) relative to Tie-2 and PDGFRα. The conservation of affinity and selectivity with the iodo (**10**) and bromo (**11**) substituted derivatives suggests tolerance towards lipophilic substitutions at the 5-indole position in most receptors tested and supports the hypothesis of the importance of electron density of the maleimide moiety to achieve good interaction at the VEGFR-2 binding site.

2.3. Radiochemistry

The radiolabeling approach was based on the general C-11 methylation reaction of the free hydroxy group[23] and was adapted for use in a commercial module (GE, Münster, Germany). Carbon-11 methyl iodide was prepared according to well documented procedures.[24] [^{11}C]CO_2 was trapped and reacted with $LiAlH_4$ in the first reactor. THF was evaporated, aqueous HI added and [^{11}C]CH_3I distilled out to the second reactor which contained

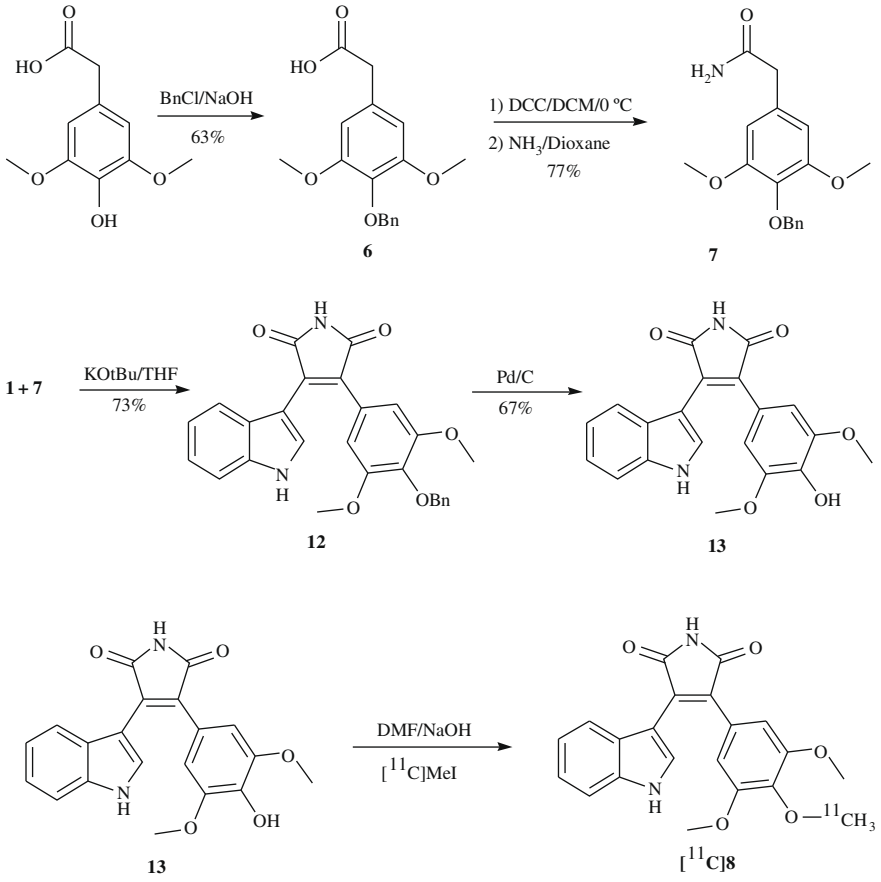

Scheme 2. Precursor synthesis and radiochemical transformation.

Table 1
Evaluation of median inhibitory concentration (IC_{50}) values for inhibition of receptor phosphorylation ($n = 3$)

Kinase	Maleimide[a] 8	Selectivity	F-Maleimide[a] 9	Selectivity	I-Maleimide[a] 10	Selectivity	Br-Maleimide[a] 11	Selectivity
EGF-R	10,133	394	>8480	>103	1688	148	5797	257
ERBB2	13,100	510	>8480	>103	15,180	609	13,316	590
IGF1-R	6967	270	8533	104	3198	128	4241	188
KIT	1900	74	3467	42	3330	133	3219	142
PDGFR-α	943	36	1800	**21**	1307	52	1156	51
PDGFR-β	1867	72	2667	32	858	34	900	40
TIE2	2633	102	1567	**19**	3961	159	2367	105
VEGF-R1	**55**	**2.14**	**150**	**1.83**	**69.4**	**2.78**	**72.4**	**3.2**
VEGF-R2	**26**	**1.00**	**82**	**1.00**	**24.89**	**1.00**	**22.5**	**1.00**
VEGF-R3	**22**	**0.87**	**66**	**0.80**	**29.51**	**1.18**	**21**	**0.93**

[a] All IC_{50} values are given in nM.

5–7 mg of the precursor **13** in a dimethylformamide/NaOH solution at −15 °C (Scheme 2). The methylation reaction took place at 80 °C for 5 min, after which 1:1 CH_3CN/H_2O was added and the crude mixture was purified by a built-in RP-HPLC to yield the final product. The desired fraction was collected into a flask containing water and loaded onto a C-18 cartridge which was washed with water and eluted with ethanol and saline to give **[^{11}C]8** in a 10% ethanol/saline solution. EOB decay corrected radiochemical yield was 20 ± 2% ($n = 5$) with a total synthesis time of 50 min. HPLC analysis of the product solution showed high radiochemical (~96%) and chemical purities with a specific activity of 3 ± 0.6 Ci/μmol decay corrected to EOB.

2.4. Log *D*

Targeting of the intracellular TK domain requires passage of the biomarkers through cellular membranes. Log *D* values of 1–3 are considered optimal for this purpose. Low lipophilicity may result in decreased membranal penetration while very high lipophilicity may result in trapping of the drug inside the membrane and increased non-specific binding. In molecular imaging, this type of non-specific binding results in accumulation of radioactivity in the blood pool (due to binding to blood proteins) and low signal/noise ratios in target tissues. All four compounds have estimated Log *P* values of 1.5–2.8, falling well within the optimal range.

The estimated Log *P* of compound **8** was calculated to be ~1.5; this projects a ratio of radioactivity of 30:1 between aqueous and octanol phases. In order to compensate for this high ratio and decrease the error in measurement of very small quantities of radioactivity in the octanol phase, we worked with a 5:1 ratio of octanol: phosphate buffer (pH 7.4, 100 mM). The measured Log $D_{7.4}$ of compound **[^{11}C]8** was found to be 1.99 ± 0.04 ($n = 4$).

2.5. In vitro blood stability

[^{11}C]8 was incubated with blood samples at 37 °C for different time periods (0, 30 and 60 min). Blood samples were centrifuged to separate pellet from plasma and the plasma was extracted with THF/ACN (30:70). The extracted radioactivity was analyzed using both RP-HPLC (data not shown) and RP-TLC plates where radioactive bands were visualized using a phosphor image plate. The average extracted radioactivity was 68%, 61% and 62% for 0, 30, and 60 min incubation, respectively. Formation of radioactive metabolites was extremely low ($n = 3$).

2.6. Specific binding studies of [^{11}C]8 in intact 293/KDR cells

As a candidate bioprobe for tracking changes in expression of VEGFR-2 in tumors, **[^{11}C]8** must offer adequate levels of specific binding (SB) to the receptor. **[^{11}C]8** was incubated with or without an excess of compound **8** in order to measure non-specific binding (NSB) and total binding (TB), respectively. Cell-bound radioactivity was separated from free radioactivity, measured in a γ-counter and SB was calculated by deducting the NSB from the TB. As illustrated in Figure 1, SB of 72% and 68% of TB was attained at 10 and 20 nM of **[^{11}C]8**, respectively.

2.7. Development of tumor-bearing animal xenograft models

Tumor-bearing animal models were analyzed using several parameters. Nude mice were inoculated subcutaneously either with 1.5–2 × 10^6 for 7–21 days for the 293/KDR cells or with 1.5–4 × 10^6 for 4–20 days for the U87MG.wt EGFR cells. Cells were implanted with or without Matrigel. Histopathological confirmation of tumor model applicability was performed via evaluation of mitosis as an indication for proliferation, necrosis, inflammation as indicated by the presence of neutrophils, lymphocytes, etc., and vascularity, associated with VEGFR-2 presence. VEGFR-2 expression in tumors and surrounding vasculature was estimated using immunohistochemistry (Fig. 2). The most favorable results obtained with 21-day U87MG.wt EGFR (1.5 × 10^6 cells) and 7-day 293/KDR (2 × 10^6 cells) tumors are described in Table 2.

In addition to the immunohistochemical results, Western blot analysis was used to evaluate VEGFR-2 expression in the different tumors. Both U87MG.wt EGFR and 293/KDR tumors had a statistically different expression of VEGFR-2 in comparison to U138 and HEK tumors which are known to express lower levels of VEGFR-2. No statistical difference was found when comparing VEGFR-2 expression in the 293/KDR and U87MG.wt EGFR (Fig. 3).

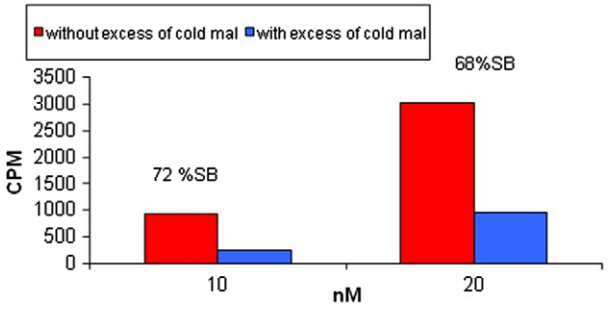

Figure 1. Specific binding of **[^{11}C]8** to 293/KDR cells. Cells were incubated either with or without excess of cold compound **8**. 10 or 20 nM **[^{11}C]8** was added for incubation, cell bound activity separated and binding quantified using a γ-counter. Specific binding was determined by subtracting the bound activity with an excess of **8** measurements (blue) from the one without an excess of **8** (red).

2.8. [^{11}C]8 Biodistribution studies in tumor-bearing mice

The in vivo distribution of **[^{11}C]8** in tumor-bearing mice was assessed at 30 and 60 min post injection. Comparison of the percentages of injected dose per gram of organ obtained for the 293/KDR and U87MG.wt EGFR models are presented in Table 3. Activity uptake levels of all organs except for liver declined by approximately 50% between 30 and 60 min post injection. Both tumors underwent rapid washout of activity between the time points examined with neither surpassing activity in the blood, indicating a lack of tracer accumulation in tumor tissue. The highest levels of activity uptake were observed in the liver and kidneys however while the kidneys underwent rapid washout of activity, liver activity was maintained over 60 min, reaching up to a 21-fold ratio with respect to tumors.

2.9. In vitro hepatic microsome stability

[^{11}C]8 was incubated with hepatic microsomes at 37 °C for different time periods (0, 15, 30 and 60 min). Samples were loaded onto a celite plug and activity eluted with ethanol. The ethanol solution was analyzed using RP-HPLC (data not shown). The percent of intact **[^{11}C]8** was found to be 96%, 40%, 25%, and 16% at 0, 15, 30 and 45 min, respectively. Two major metabolites were formed, both highly polar in nature.

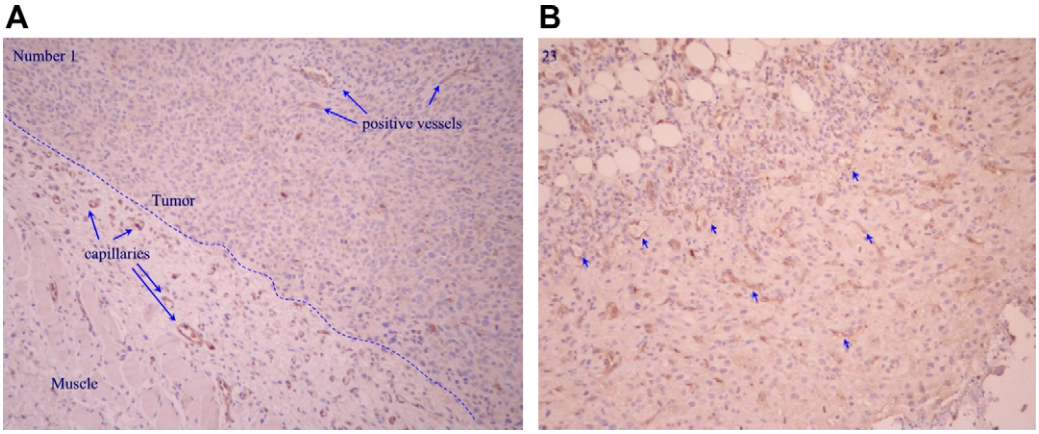

Figure 2. Immunohistochemical staining of 293/KDR (A) and U87MG.wt EGFR (B) for the expression of VEGFR-2, confirming VEGFR-2 expression in both tumor models.

Table 2
Validation of human tumor xenografts in nude mice, by histopathology and immunohistochemistry[a]

Tumor model	Volume (cm^3)	Necrosis(%)[b]	Mitosis per HPF	Inflammation[c]	Vessels per HPF	VEGFR capillaries	VEGFR vessels	VEGFR tumor cells
293/KDR	0.22 ± 0.13 (n = 11)	16 ± 9 (n = 11)	1.8 ± 0.4 (n = 11)	1.5 ± 0.3 (n = 4)	4.7 ± 0.6 (n = 7)	1.5 ± 0.4 (n = 11)	2.3 ± 0.5 (n = 11)	2.6 ± 0.2 (n = 11)
U87MG.wt EGFR	0.09 ± 0.02 (n = 7)	33 ± 15 (n = 7)	2.8 ± 0.4 (n = 6)	1.6 ± 0.3 (n = 7)	7.0 ± 1.4 (n = 3)	1.9 ± 0.8 (n = 7)	5.3 ± 2.4 (n = 5)	2.6 ± 0.6 (n = 7)

[a] Results are presented as mean ± SEM.
[b] The percentage of necrosis is approximate.
[c] The inflammation is scored using semi-quantitative grading (0–4).

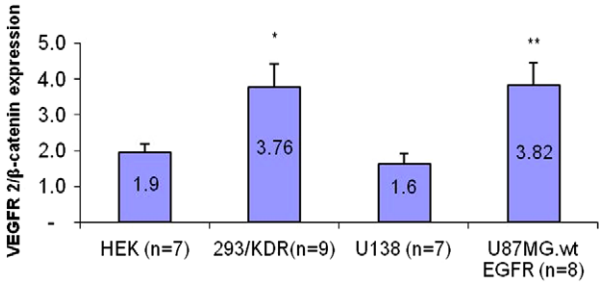

Figure 3. The expression of VEGFR-2 in 293/KDR and U87MG.wt EGFR tumors was statistically different from HEK (p = 0.03) and U138 (p = 0.009) tumors, respectively. No statistically difference was found comparing VEGFR-2 expression in the 293/KDR and U87MG.wt EGFR.

3. Conclusion

The obtained data in this study indicate that three out of the four diarylmaleimide derivatives synthesized exhibited high affinity and selectivity towards the VEGF family of receptors. The fluoro derivative showed decreased selectivity as compared to PDGFRα and TIE2. All four derivatives can easily be labeled with carbon-11 and have appropriate Log *P* values for PET bioprobe development. In addition, the lead compound **[^{11}C]8** had specific binding in cells overexpressing VEGFR-2 and was stable in human blood. Unfortunately, biodistribution studies performed in tumor-bearing mice with the labeled lead structure showed neither high accumulation nor retention of the bioprobe in target tissues. The low stability of these compounds to liver enzyme metabolism may hamper future development as PET tracers; thus, the maleimide moiety, known to have high affinity to sulfhydryl functions, may be at fault, requiring a different connecting group (e.g., triazole) as replacement.

4. Materials and methods

4.1. General methods

All operations with air- and moisture-sensitive compounds were performed by the Schlenk techniques under argon atmosphere. All solvents were of analytical grade or better. Tetrahydrofuran (THF) was distilled over sodium/benzophenone; other solvents were purchased as anhydrous. ^{1}H NMR spectra were recorded on a 300 MHz spectrometer in DMSO-d_6 or $CDCl_3$. ^{1}H signals are reported in ppm. ^{1}H NMR signals are referenced to the residual proton (7.26 and 2.50 ppm for $CDCl_3$ and DMSO-d_6, respectively) of a deuterated solvent. Mass spectra were obtained on a spectrometer equipped with CI, EI, and FAB probes and on a spectrometer equipped with an ESI probe. HRMS results were obtained on MALDI-TOF and ESI mass spectrometers. Flash chromatography was carried out on SiO_2 (0.04–0.063 mm). HPLC was performed on a system with a variable wavelength detector operating at 254 nm and a radioactivity detector with a NaI crystal. Two HPLC systems were used: (A) a reversed-phase system employing a Macherey–Nagel column (C18, Nucleosil, 7 μm, 250· 16 mm) and 42% CH_3CN/58% acetate buffer 0.1 M/pH 3.8 as eluent, at a flow rate of 12 mL/min installed in the carbon-11 module. (B) Analysis of formulated radiotracer was performed on a reversed-phase system using a Waters column (C18, μBondapak, 10 μm, 125A, 300· 3.9 mm) and 42% CH_3CN/58% acetate buffer 0.1 M/pH 3.8 as solvents at a flow rate of 1 mL/min, rt = 12 min.

Radiosyntheses were carried out on a [^{11}C]CH_3I module (GE, Münster, Germany). Specific radioactivities were determined by HPLC, using cold mass calibration curves. [^{11}C]CO_2 was produced by the ^{14}N(p,α)^{11}C nuclear reaction on nitrogen containing 0.5% oxygen, using an 18/9 IBA cyclotron. Bombardment was carried out for 40 min with a beam of 16-MeV protons. At the end of bombardment (EOB), the target gas was delivered and trapped by a cryogenic trap in the [^{11}C]CH_3I module.

All IC_{50} studies were performed by ProQinase GmbH (Freiburg, Germany).

4.2. Chemistry and radiochemistry

4.2.1. Methyl 2-(1*H*-indol-3-yl)-2-oxoacetate (1)[22]

Oxalyl chloride (0.86 mL, 10 mmol) was added dropwise to a solution of 1*H*-indole (1.17 g, 10 mmol) in diethyl ether (12 mL) cooled in an ice bath. The reaction mixture kept stirring under the same conditions for 30 min, cooled to −65 °C and a 25 wt % solution of CH_3ONa in MeOH (4.7 mL, 23 mmol) was added dropwise. The reaction mixture was warmed to room temperature, stirred for an additional 30 min and quenched by adding water (18 mL). The product was isolated by filtration, washed with dichloromethane (DCM) and dried to give 1.73 g of yellow solid (yield 85%). ^{1}H NMR (DMSO-

Table 3
Biodistribution of **[^{11}C]8** in 293/KDR and U87MG.wt EGFR tumor-bearing mice

%ID/g (mean ± SEM)	30 min (n = 10)	60 min (n = 10)		30 min (n = 12)	60 min (n = 10)
Blood	0.38 ± 0.04	0.29 ± 0.04	Blood	0.36 ± 0.03	0.19 ± 0.04
U87MG.wtEGFR	0.33 ± 0.08	0.17 ± 0.03	293/KDR	0.30 ± 0.03	0.14 ± 0.03
Skin	0.41 ± 0.06	0.21 ± 0.04	Skin	0.38 ± 0.03	0.14 ± 0.04
Bone	0.19 ± 0.03	0.11 ± 0.02	Bone	0.15 ± 0.02	0.09 ± 0.02
Muscle	0.17 ± 0.03	0.09 ± 0.02	Muscle	0.20 ± 0.02	0.08 ± 0.02
Liver	2.64 ± 0.29	1.68 ± 0.51	Liver	2.89 ± 0.22	2.95 ± 1.18
Kidney	2.24 ± 0.23	0.79 ± 0.17	Kidney	2.29 ± 0.16	0.80 ± 0.27

d_6): δ 12.40 (br s, 1H), 8.42 (d, *J* = 3.3, 1H), 8.15 (s, 1H), 7.51 (s, 1H) 7.26 (m, 2H), 3.87 (s, 3H); MS (ESI, *m/z*): 204 (M^++1).

4.2.2. Methyl 2-(5-fluoro-1*H*-indol-3-yl)-2-oxoacetate (2)

Material synthesized as **1** with 5-fluoro-1*H*-indole (810 mg, 6 mmol), diethylether (8 mL), oxalyl chloride (0.52 mL, 6 mmol) and CH_3ONa solution (2.8 mL, 13.7 mmol) to give 1.08 g of yellow solid (yield 82%). ^{1}H NMR (DMSO-d_6): δ 8.54 (d, *J* = 3.6, 1H), 7.4 (dd, *J* = 2.4, *J* = 9.6, 1H), 7.53–7.59 (q, *J* = 4.5, 1H), 7.12–7.19 (m, 1H), 3.89 (s, 3H); MS (ESI, *m/z*): 222 (M^++1).

4.2.3. Methyl 2-(5-iodo-1*H*-indol-3-yl)-2-oxoacetate (3)

Material synthesized as **1** with 5-iodo-1*H*-indole (729 mg, 3 mmol), diethylether (5 mL), oxalyl chloride (0.27 mL, 3 mmol) and CH_3ONa solution (1.4 mL, 6.8 mmol) to give 553 mg of yellow solid (yield 56%). ^{1}H NMR (DMSO-d_6): δ 8.5 (s, 1H) 8.46 (d, *J* = 3.3, 1H), 7.59 (d, *J* = 8.4, 1H), 7.4 (d, *J* = 8.7, 1H), 3.89 (s, 3H); MS (ESI, *m/z*): 329 (M^++1).

4.2.4. Methyl 2-(5-bromo-1*H*-indol-3-yl)-2-oxoacetate (4)

Material synthesized as **1** with 5-bromo-1*H*-indole (588 mg, 3 mmol), diethylether (5 mL), oxalyl chloride (0.27 mL, 3 mmol) and CH_3ONa solution (1.4 mL, 6.8 mmol) to give 572 mg of yellow solid (yield 68%). ^{1}H NMR (DMSO-d_6): δ 8.51 (d, *J* = 3.3, 1H), 8.28 (s, 1H), 7.53 (d, *J* = 8.7, 1H), 7.44 (d, *J* = 8.7, 1H), 3.89 (s, 3H); MS (ESI, *m/z*): 282 (M^++1).

4.2.5. 2-(3,4,5-Trimethoxy-phenyl) acetamide (5)

A solution of 2-(3,4,5-trimethoxyphenyl)acetic acid (1 g, 4.4 mmol) in DCM (30 mL) was added dropwise to a solution of *N,N′*-dicyclohexylcarbodiimide (DCC) (1.1 g, 5.3 mmol) in DCM (15 mL) cooled to 0 °C. The reaction mixture was stirred at 0 °C for 1 h and a 0.5 M solution of NH_3 in dioxane (17.6 mL, 8.8 mmol) was added and stirring was continued at room temperature overnight. The reaction mixture was filtered, solvent was evaporated and the product was purified via column chromatography with ethyl acetate as eluent to give 790 mg of white solid (yield 80%). ^{1}H NMR ($CDCl_3$): δ 6.48 (s, 2H), 5.2 (d, *J* = 9, 2H), 3.86 (s, 6H), 3.84 (s, 3H), 3.53 (s, 2H); MS (ESI, *m/z*): 226 (M^++1).

4.2.6. 2-(4-Benzyloxy-3,5-dimethoxyphenyl) acetic acid (6)

2-(4-Hydroxy-3,5-dimethoxyphenyl) acetic acid (1 g, 4.7 mmol) was dissolved in a solution of THF, 2 M NaOH (12.5 mL, 1:1.5) and benzyl chloride (0.64 mL, 5.6 mmol) was added. The reaction mixture was refluxed overnight, THF was evaporated and the reaction acidified to pH 1 using concentrated HCl. The white precipitate which formed was extracted with DCM, the organic phases united and washed with 5% HCl and brine and dried over Na_2SO_4. The product was purified via column chromatography with 2% MeOH in DCM as eluent to give 0.9 g of white solid (yield 63%). ^{1}H NMR ($CDCl_3$): δ 7.47 (d, *J* = 9.3, 2H), 7.32 (m, 3H), 6.49 (s, 2H), 4.97 (s, 2H), 3.81 (s, 6H), 3.58 (s, 2H); MS (ESI, *m/z*): 303 (M^++1).

4.2.7. 2-(4-Benzyloxy-3,5-dimethoxyphenyl) acetamide (7)

The title compound was synthesized under the same conditions as **5** using **6** (604 mg, 2 mmol), DCC (500 mg, 2.4 mmol), DCM (30 mL) and a 0.5 M solution of NH_3 in dioxane (8 mL, 4 mmol). Column chromatography with a gradient of 0–4% MeOH in DCM gave 465 mg of white solid (yield 77%). ^{1}H NMR ($CDCl_3$): δ 7.47 (d, *J* = 9.3, 2H), 7.32 (m, 3H), 6.49 (s, 2H), 5.77 (d, *J* = 5.7, 2H), 4.94 (s, 2H), 3.77 (s, 6H), 3.46 (s, 2H); MS (ESI, *m/z*): 302 (M^++1).

4.2.8. 3-(1*H*-Indol-3-yl)-4-(3,4,5-trimethoxyphenyl)-1*H*-pyrrole-2,5-dione (8)[21]

A stirred solution of the amide **5** (100 mg, 0.44 mmol) and indole **1** (181 mg 0.88 mmol) in dry THF containing 30 mg of molecular sieves (4 Å) was cooled to 0 °C under nitrogen atmosphere. A solution of potassium tert-butoxide (KO*t*Bu) (1 M, 2.1 mmol) was added dropwise during which time the reaction color changed to purple. The reaction mixture was stirred overnight at room temperature and quenched by addition of a saturated solution of NH_4Cl. The THF phase was separated, the aqueous phase extracted with EtOAc and the organic phases united, dried over Na_2SO_4 and the product purified via flash column chromatography using 2% MeOH in DCM to give 131 mg of orange solid (yield 79%). ^{1}H NMR (DMSO-d_6): δ 12.00 (s, 1H), 11.14 (s, 1H), 8.08 (s, 1H), 7.56 (d, *J* = 7.8, 1H), 7.16 (t, *J* = 7.5, 1H), 6.84 (m, 3H), 6.45 (d, *J* = 7.8, 1H), 3.76 (s, 3H), 3.48 (s, 6H); HRMS 379.1322 (M+1, calcd 379.1294).

4.2.9. 3-(5-Fluoro-1*H*-indol-3-yl)-4-(3,4,5-trimethoxyphenyl)-1*H*-pyrrole-2,5-dione (9)

The title compound was synthesized as described for **8** using amide **5** (100 mg, 0.44 mmol) and indole **2** (195 mg, 0.88 mmol). Flash column chromatography using a gradient of 1–2% MeOH in DCM gave 144 mg of orange solid (yield 83%). ^{1}H NMR (DMSO-d_6): δ 12.11 (s, 1H), 11.18 (s, 1H), 8.16 (s, 1H), 7.56 (m, 1H), 7.04 (m, 1H), 6.81 (m, 2H), 6.02 (dd, *J* = 10.8, *J* = 2.7, 1H), 3.77 (s, 3H), 3.53 (s, 6H); HRMS 395.1035 (M−1, calcd 395.1043), mp 258–259 °C.

4.2.10. 3-(5-Iodo-1*H*-indol-3-yl)-4-(3,4,5-trimethoxyphenyl)-1*H*-pyrrole-2,5-dione (10)

The title compound was synthesized as described for **8** using amide **5** (100 mg, 0.44 mmol) and indole **3** (290 mg, 0.88 mmol). Flash column chromatography using a gradient of 1–2% MeOH in DCM gave 146 mg of orange solid (yield 66%).^{1}H NMR (DMSO-d_6): δ 12.05 (s, 1H), 11.07 (s, 1H), 8.00 (s, 1H), 7.31 (m, 2H), 6.68 (s, 2H), 6.64 (s, 1H), 3.77 (s, 3H), 3.53 (s, 6H); HRMS 503.0128 (M−1, calcd 503.0104), mp 285 °C (decomposition).

4.2.11. 3-(5-Bromo-1*H*-indol-3-yl)-4-(3,4,5-trimethoxyphenyl)-1*H*-pyrrole-2,5-dione (11)

The title compound was synthesized as described for **8** using amide **5** (100 mg, 0.44 mmol) and indole **4** (248 mg, 0.88 mmol). Flash column chromatography using a gradient of 1–2% MeOH in DCM gave 110 mg of orange solid (yield 55%). ^{1}H NMR (DMSO-d_6): δ 12.09 (s, 1H), 11.10 (s, 1H), 8.07 (s, 1H), 7.42 (d, *J* = 8.4, 1H), 7.31 (d, *J* = 10.5, 1H), 6.70 (s, 2H), 6.37 (s, 1H), 3.75 (s, 3H), 3.46 (s, 6H); HRMS 455.0225 (M−1, calcd 455.0243), 459 (M^++1), mp 267 °C (decomposition).

4.2.12. 3-(4-Benzyloxy-3,5-dimethoxyphenyl)-4-(1*H*-indol-3-yl)-1*H*-pyrrole-2,5-dione (12)

The title compound was synthesized as described for **8** using amide **7** (435 mg, 1.5 mmol), indole **1** (611 mg, 3 mmol), THF (42 mL), molecular sieves (100 mg) and KO*t*Bu (7 mL, 7 mmol). Flash column chromatography using 1% MeOH in DCM as eluent produced 500 mg of orange solid (yield 73%). ^{1}H NMR (DMSO-d_6): δ 11.9 (s, 1H), 11.04 (s, 1H), 7.98 (s, 1H), 7.31–7.47 (m, 5H), 7.09 (t, *J* = 7.8, 1H), 6.74–6.79 (m, 3H), 6.37 (d, 1H), 4.92 (s, 2H), 3.38 (s, 6H); MS (ESI, *m/z*): 455 (M^++1).

4.2.13. 3-(4-Hydroxy-3,5-dimethoxyphenyl)-4-(1*H*-indol-3-yl)-1*H*-pyrrole-2,5-dione (13)

Compound **12** (84 mg, 0.185 mmol) was dissolved in a MeOH:THF solution (6:1, 14 mL) and Pd/C (10%, 8.5 mg) was added. The hydrogenation was performed at 4 psi for 2 h. The reaction mixture was filtered and evaporated to give a reddish solid which was purified via flash column chromatography with 1% MeOH in DCM as eluent to give 45 mg of red solid (yield 67%). ^{1}H NMR (DMSO-d_6): δ 11.84 (s, 1H), 10.97 (s, 1H), 8.8 (s, 1H),

7.91 (d, J = 4.5, 1H), 7.42 (d, J = 8.1, 1H), 7.06 (t, J = 7.5, 1H), 6.74–6.78 (m, 3H), 6.45 (d, J = 7.8, 1H), 3.39 (s, 6H); MS (ESI, m/z): 365 (M^++1).

4.2.14. 3-(1*H*-Indol-3-yl)-4-(3,5-dimethoxy-4-[^{11}C]methoxyphenyl)-1*H*-pyrrole-2,5-dione ([^{11}C]8)

The synthesis and use of [^{11}C]MeI was published in the past.[24] Briefly, [^{11}C]CO_2 (1117 ± 72 mCi, 41 ± 2.6 GBq) was trapped at −160 °C. The temperature of the cooling trap was increased to −20 °C, and the activity was transferred by a stream of argon (20 mL/min) into a reactor containing 300 μL of 0.25 N $LiAlH_4$ in THF at −50 °C. After 90 s, the solvent was removed under reduced pressure. In this manner, more than 70% of the activity was recovered. The reactor temperature was increased to 160 °C, HI was added and [^{11}C]MeI was distilled (argon flow of 25 mL/min) through a NaOH column to a second reactor, containing the 5 mg of **13** in a solution of dimethylformamide (600 μL) and NaOH (5 M, 20 μL) at −15 °C. After 1 min of distillation, an average of 502 ± 54 mCi (18.5 ± 2 GBq) (n = 5) was trapped in the second reactor. The reactor was sealed and heated to 80 °C for 5 min. At the end of the 5 min reaction, the mixture was cooled to 40 °C, 1.2 mL of CH_3CN/H_2O (1:1) was added and the crude product was automatically injected to HPLC system A, rt = 14.5 min. The labeled product was collected in a flask containing 45 mL of water. The solution was loaded onto a C-18 cartridge (Waters Sep-Pak Plus, preactivated with 5 mL ethanol and 10 mL of water) and then washed with water (4 mL). The product was eluted with 1 mL of ethanol, followed by 9 mL of saline and collected into the product vial after a total radiosynthesis time of 50 min, with total activity of 42 ± 4 mCi (1.5 ± 0.15 GBq) and radiochemical yield of 20 ± 2% decay corrected to EOB (n = 5). Identification of the products (via coinjection) and determination of chemical, radiochemical purities (~96%) and specific activities (3 ± 0.6 Ci/μmol decay corrected to EOB) were obtained by reverse-phase HPLC on a C-18 analytical column in comparison to the standard using system B.

4.3. Evaluation of median inhibitory concentration (IC_{50}) values for inhibition of 10 tyrosine kinases

A radiometric protein kinase assay (33PanQinase® Activity Assay) was used for measuring the kinase activity of the 10 protein kinases. All kinase assays were performed in 96-well FlashPlatesTM from Perkin Elmer/NEN (Boston, MA, USA) in a 50 μL reaction volume.

The assay for all enzymes contained 60 mM HEPES–NaOH, pH 7.5, 3 mM $MgCl_2$, 3 mM $MnCl_2$, 3 μM Na-orthovanadate, 1.2 mM DTT, 50 μg/mL PEG_{20000}, 1 μM [γ-^{33}P]-ATP (approx. 5×10^5 cpm per well). Depending on the kinase, the following substrate proteins were used Tie-2, PDGFRα and PDGFRβ (Poly(Ala, Glu, Lys, Tyr)$_{6:2:5:1}$), EGFR, ERBB2, IGF1-R, KIT, VEGFR-1, VEGFR-2, VEGFR-3 (Poly(Glu, Tyr)$_{4:1}$)

The IC_{50} values were measured by testing 12 concentrations of compounds in triplicate. As a parameter for assay quality, the Z′-factor for the low and high controls of each assay plate (n = 8) was used. The final DMSO concentration in the assay was 1%. The reaction cocktails were incubated at 30 °C for 80 min. The reaction was stopped with 50 μL of 2% H_3PO_4, plates were aspirated and washed two times with 200 μL of 0.9% NaCl. Incorporation of $^{33}P_i$ was determined with a microplate scintillation counter (Microbeta Trilux, Wallac). All assays were performed with a BeckmanCoulter/Sagian robotic system.

4.4. Log $D_{7.4}$ evaluation

For this specific experiment, **[^{11}C]8** was eluted from the C18 sep-pak with n-octanol (5 mL) instead of ethanol/saline. Approximately 200 μCi (7.4 MBq) were taken from the mother solution, transferred to a 10 mL V-vial and the volume was corrected to 5 mL with n-octanol. Phosphate buffer (1 mL, pH 7.4, 100 mM) was added and the solution was vortexed for 2 min. The two phases were separated and measured for activity. Log $D_{7.4}$ was calculated as 1.99 ± 0.04 (n = 4).

4.5. In vitro blood stability

Fresh human blood samples were collected in a Vacutainer™ containing EDTA (K3, BD, USA), divided into 1 mL aliquots and incubated for 15 min at 37 °C with gentle shaking. Approximately 300 μCi of **[^{11}C]8** solution was added to blood samples for 0, 30 or 60 min, after which the samples were removed from the incubator and centrifuged at 3500 rpm for 5 min. The plasma was separated from the precipitant and radioactivity levels were measured for both fractions in a dose calibrator (CRC-35, Capintec, Canada). 1.2 mL of cold THF/ACN (30:70) solution was added to the plasma fraction; the plasma was vortexed for 30 s and then centrifuged again for 5 min at 10,600 rcf (g) and pellet and plasma were separated and measured for radioactivity levels. The protein-free plasma was then filtered through a 0.45 μm filter (Puradisc, Whatman) and samples were both injected into RP-HPLC (results not shown) and loaded on a TLC plate (Partisil LKC18F silica gel 5 × 20 cm, 200 μm layer thickness, Whatman). TLC plates were run with 40:60 H_2O:ACN as a mobile phase and exposed for 1 h to phosphor imager plates (BAS–IP MS 2040 Fuji Photo Film Co. Ltd) for visualization of radioactive bands (Fig. 4). The plates were scanned with a BAS reader 3.1 version scanner and analyzed with TINA 2.10 software.

4.6. Cell culture

Human glioma cell line U87MG.wt EGFR and U138 human glioma cell line, were grown as described previously.[25] 293 Human kidney cells expressing VEGFR-2 (293/KDR, SibTech, Brookfield, CT) and 293 Human embryonic kidney (HEK) wt cells were grown in Dulbecco's Modified Eagle's Medium (DMEM; Renium, Israel) supplemented with 10% fetal calf serum (FCS) and anti-biotics (10^5 U/L penicillin and 100 mg/L streptomycin) at 37 °C in 5% CO_2.

4.7. Specific binding studies of [^{11}C]8 in intact 293/KDR cells

The receptor-binding properties of **[^{11}C]8** to VEGFR-2 were evaluated in a direct radioligand binding assay using 293/KDR cells (2×10^6 VEGFR-2/cell). 293/KDR cells were suspended in PBS (1×10^6 cells/ml/microtube), and incubated at 4 °C for 30 min with gentle agitation. To measure non-specific binding (NSB), one set of microtubes was incubated with excess of non-labeled VEGFR-2 inhibitor (compound **8**, 32 μM, 0.5% DMSO, 0.1% ethanol, 30 min). To measure the total binding (TB), a matching set of microtubes was incubated with 0.5% DMSO and 0.1% ethanol vehicle. **[^{11}C]8** (3.15 Ci/μmol, 0.5% ethanol final concn) was then added to the microtubes at two concentrations (10, 20 nM) for 30 min. For each concentration of **[^{11}C]8** that was added to the cells, a corresponding control sample, consisting of cell-free PBS, was incubated with the same concentration of the labeled inhibitor so as to calculate the cell-independent retention of activity by the test microtubes. Cell-bound radioactivity was separated from free radioactivity by centrifugation at 2700g, 4 °C for 5 min, followed by washing with PBS. Microtubes were measured for their radioactive content using a γ-counter (1480 Wizard 3″). Values obtained (in cpm) were corrected for the cell-independent microtube retention of activity by deducting the signals of the control samples. Specific binding (SB) was calculated by subtracting the NSB from the corresponding TB at each concentration.[26]

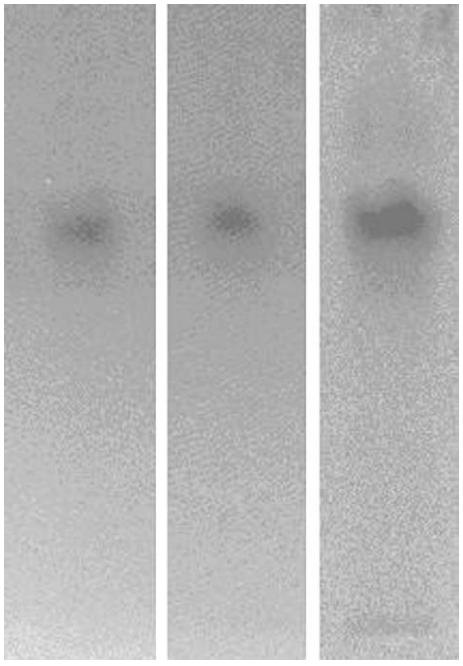

Figure 4. TLC of the radioactive metabolites extracted from blood samples at 0, 30, and 60 min (left to right, respectively) showing only one major spot.

4.8. Animal studies

Nude Hsd-Athymic Nude-nu male mice (7–8 weeks, 25–30 g) were obtained from Harlan Industries, Inc. All animal studies were conducted under a protocol approved by the Research Animal Ethics Committee of the Hebrew University of Jerusalem and in accordance with its guidelines. Mice were allowed to acclimate in the animal facility for at least 3 days prior to their inoculation with tumor cells. They were routinely kept in 12-h light/dark cycles and provided with food and water ad libitum.

4.9. Development of tumor-bearing animal xenograft models of 293/KDR and human glioma U87MG.wt EGFR

293 Human kidney expressing VEGFR-2 (293/KDR), 293 Human Embryonic Kidney (HEK) wt, human glioma U87MG.wt EGFR and U138MG cells were cultured in vitro as described above. Subconfluent cultures were released from the flasks with trypsin, counted with a hemocytometer using trypan blue and suspended in DMEM medium. U87MG.wt EGFR cell suspensions were supplemented with Matrigel (20% vol/vol; BD Biosciences, Biological Industries, Israel) and thoroughly mixed prior to their injection into mice. Mice were inoculated subcutaneously with $1.5–2 \times 10^6$ for 7–21 days for the 293/KDR cells, with 5×10^6 for 7–10 days for the HEK cells, with $1.5–4 \times 10^6$ for 4–20 days for the U87MG.wt EGFR cells and with $2–2.5 \times 10^6$ for 7–13 days for the U138 cells. All inoculations were in a volume of 100 μL.

4.10. Histology and immunohistochemistry

Histological and immunohistochemical validation of tumor models was performed by Patho-Lab Ltd (Rehovot, Israel). Tumors were generated as described above. Tumor specimens were fixed in 4% formalin and delivered to Patho-Lab Ltd for further treatment. Briefly, tumor samples were paraffin embedded, serial paraffin sections of the tumors were deparaffinized and rehydrated, and endogenous peroxidase activity was quenched by immersing the sections in 3% H_2O_2 for 10 min, followed by treatment with a pressure cooker for 12 min in a Nuclear Decloaker solution (pH 9). The tumor sections were incubated with primary antibody specific for VEGFR-2 (rabbit monoclonal anti-VEGFR-2, 1:100, Cell Signaling Technology, Boston, MA) for 1 h in a humidifier chamber. Slides were washed in PBS and incubated for 5 min with Zymed DAB staining kit. Negative control staining was carried out by omitting primary antibody. Finally, tissue sections were counterstained with hematoxylin and coverslipped.

4.11. VEGFR extraction from tumors

Tumors were collected from mice, placed immediately in liquid nitrogen and kept at −170 °C until VEGFR extraction. Prior to the extraction, tumors were weighed and homogenized on ice (Omni tip, US) in 2 mL/100 mg of lysis buffer (50 mM Tris–HCl; 1% NP-40; 0.25% Na-deoxycholate; 150 mM NaCl, 1 mM EDTA; 1 mM NaF; 1 mM Na_3VO_4 and 1% protease inhibitor). After homogenization samples were centrifuged (15 min; 4 °C; 14,000 rpm) to allow separation of pellet and supernatant. The supernatant (containing VEGFR-2) was diluted (3:1) with Laemmli sample buffer (Bio-Rad, Israel) and boiled for 10 min at 100 °C to allow for western blot analysis. Protein amounts of the samples were measured by Qubit fluorometer.

4.12. Western blot

Equal amounts of protein lysates (300 μg) were loaded and separated by sodium dodecyl sulfate polyacrylamide gel (SDS–PAGE, Bio-Rad) and electrophoretically transferred to a nitrocellulose membrane. The membrane was blocked in 5% low fat dehydrated milk (BD) in TBST buffer (10 mM Tris–HCl, pH 7.4, 0.05% Tween 20) for 120 min, and then probed overnight at 4 °C with the following primary antibodies diluted in blocking TBST: (I) rabbit polyclonal anti-Flk-1 (VEGFR-2), 1:1000 dilution (Santa Cruz Biotechnology Inc.) and (II) mouse monoclonal anti-β-catenin, 1:200 dilution (Santa Cruz Biotechnology Inc.). The membrane was washed thoroughly with TBST and incubated for 1 h at room temperature, with a horseradish peroxidase—conjugated anti-mouse IgG (1:5000 dilution in blocking TBST). Finally, the membrane was washed in TBST (4×5 min), and immunoreactive proteins were visualized using an enhanced chemiluminescence (ECL, PIR34080 pierce) detection reagent, and exposed to a FUGI medical X-ray film (FUJIFILM Corporation, Tokyo).

The films were scanned with a BAS reader 3.1 version scanner and analyzed with TINA 2.10 software. The intensity of each VEGFR-2 band was normalized to the intensity of the corresponding β-catenin band to correct for differences in the content of total protein loaded.

4.13. [^{11}C]8 Biodistribution studies in tumor-bearing mice

Biodistribution studies were carried out with Nude Hsd-Athymic Nude-nu mice (10–12 weeks old) carrying U87MG.wt EGFR or 293/KDR tumors grown as described above.

[^{11}C]8 (197 ± 16 μCi; 1.1 ± 0.3 Ci/μmol; 225 ± 11 μL) in a 10% ethanol/saline solution was injected via the lateral vein. At allotted time points (30, 60 min), blood was drawn from the orbital sinus; mice were sacrificed by cervical dislocation and selected organs (tumor, skin, bone, liver, and kidney) were excised, weighed and measured for their radioactive content using a γ-counter (1480 Wizard 3″). Distribution of activity was calculated as the percentage of injected dose per gram of organ (%ID/g). Activity uptake ratios of various organs were calculated by dividing the corresponding calculated percentages of injected dose per gram of organ.

4.14. In vitro hepatic microsome stability

Metabolism was evaluated by incubating the tracer [2–3 mCi (74-111 GBq) in 100 μL ethanol] with 0.5 mg/mL mouse hepatic microsomes (BD Biosciences) in PBS pH 7.4 at 37 °C for 5 min. The reaction was started with the addition of 0.25 mM NADPH followed by incubation in 37 °C for 0, 15, 30, and 60 min. At each time point, 300–600 μL of the mixture were removed and loaded onto a 2 cm celite plug. The plug was dried and eluted with 2 mL of ethanol. The ethanol solution was analyzed by RP-HPLC using system B.[19,27]

Acknowledgments

We would like to thank Dr. Orit Jacobson for her help with the radiochemical experiments. This research was supported by the Israel Science Foundation (Grant #445/07 to E.M.). Ohad Ilovich's research was generously supported by the Hoffman Leadership and Responsibility fund, at the Hebrew University.

References and notes

1. Pandya, N. M.; Dhalla, N. S.; Santani, D. D. *Vasc. Pharmacol.* **2006**, *44*, 265.
2. Levitzki, A.; Mishani, E. *Annu. Rev. Biochem.* **2006**, *75*, 93.
3. Fujita, Y.; Abe, R.; Shimizu, H. *Curr. Pharm. Des.* **2008**, *14*, 3820.
4. Chase, J. L. *Pharmacotherapy* **2008**, *28*, 23S.
5. Pytel, D.; Sliwinski, T.; Poplawski, T.; Ferriola, D.; Majsterek, I. *Anticancer Agents Med. Chem.* **2009**, *9*, 66.
6. Serkova, N. J.; Garg, K.; Bradshaw-Pierce, E. L. *Rec. Pat. Anticancer Drug Discovery* **2009**, *4*, 35.
7. Van de Wiele, C.; Boersma, H.; Dierckx, R. A.; De Spiegeleer, B.; Van Waarde, A.; Elsinga, P. H. *Curr. Pharm. Des.* **2008**, *14*, 3340.
8. Decristoforo, C.; Hernandez Gonzalez, I.; Carlsen, J.; Rupprich, M.; Huisman, M.; Virgolini, I.; Wester, H. J.; Haubner, R. *Eur. J. Nucl. Med. Mol. Imaging* **2008**, *35*, 1507.
9. Beer, A. J.; Schwaiger, M. *Cancer Metastasis Rev.* **2008**, *27*, 631.
10. Cai, W.; Chen, X. *J. Nucl. Med.* **2008**, *49*, 113S.
11. Kenny, L. M.; Coombes, R. C.; Oulie, I.; Contractor, K. B.; Miller, M.; Spinks, T. J.; McParland, B.; Cohen, P. S.; Hui, A. M.; Palmieri, C.; Osman, S.; Glaser, M.; Turton, D.; Al-Nahhas, A.; Aboagye, E. O. *J. Nucl. Med.* **2008**, *49*, 879.
12. Erdag, B.; Balcioglu, K. B.; Kumbasar, A.; Celikbicak, O.; Zeder-Lutz, G.; Altschuh, D.; Salih, B.; Baysal, K. *Mol. Biotechnol.* **2007**, *35*, 51.
13. Youssoufian, H.; Hicklin, D. J.; Rowinsky, E. K. *Clin. Cancer Res.* **2007**, *13*, 5544s.
14. Panares, R. L.; Garcia, A. A. *Exp. Rev. Anticancer Ther.* **2007**, *7*, 433.
15. Cai, W.; Chen, X. *Front. Biosci.* **2007**, *12*, 4267.
16. Chen, K.; Cai, W.; Li, Z. B.; Wang, H.; Chen, X. *Mol. Imaging Biol.* **2009**, *11*, 15.
17. Ilovich, O.; Jacobson, O.; Aviv, Y.; Litchi, A.; Chisin, R.; Mishani, E. *Bioorg. Med. Chem.* **2008**, *16*, 4242.
18. Ilovich, O.; Åberg, O.; Långström, B.; Mishani, E. *J. Labelled Compd. Radiopharm.* **2009**, *52*, 151.
19. Samen, E.; Thorell, J. O.; Lu, L.; Tegnebratt, T.; Holmgren, L.; Stone-Elander, S. *Eur. J. Nucl. Med. Mol. Imaging* **2009**, *36*, 1283.
20. Peifer, C.; Krasowski, A.; Hammerle, N.; Kohlbacher, O.; Dannhardt, G.; Totzke, F.; Schachtele, C.; Laufer, S. *J. Med. Chem.* **2006**, *49*, 7549.
21. Peifer, C.; Stoiber, T.; Unger, E.; Totzke, F.; Schachtele, C.; Marme, D.; Brenk, R.; Klebe, G.; Schollmeyer, D.; Dannhardt, G. *J. Med. Chem.* **2006**, *49*, 1271.
22. Faul, M. M.; Winneroski, L. L.; Krumrich, C. A. *J. Org. Chem.* **1998**, *63*, 6053.
23. Lin, K. S.; Ding, Y. S. *Chirality* **2004**, *16*, 475.
24. Crouzel, C.; Långström, B.; Pike, V. W.; Coenen, H. H. *Int. J. Radiat. Appl. Inst. Part A Appl. Radiat. Isot.* **1987**, *38*, 601.
25. Abourbeh, G.; Dissoki, S.; Jacobson, O.; Litchi, A.; Ben Daniel, R.; Laki, D.; Levitzki, A.; Mishani, E. *Nucl. Med. Biol.* **2007**, *34*, 55.
26. de Lemos Rieper, C.; Galle, P.; Svenson, M.; Pedersen, B. K.; Hansen, M. B. *J. Immunol. Methods* **2009**, *350*, 46.
27. Lee, S. Y.; Choe, Y. S.; Kim, D. H.; Park, B. N.; Kim, S. E.; Choi, Y.; Lee, K. H.; Lee, J.; Kim, B. T. *Nucl. Med. Biol.* **2001**, *28*, 391.